An extremely high rate Li–S battery with hybrid electrolyte

Y.-H. Xu, Q.-F. Zhang, B Fan, B Xue, H.-J. Chen, Xianghua Zhang, Z.-K. Luo, F. Wang, David Le Coq, Laurent Calvez, et al.

▶ **To cite this version:**

Y.-H. Xu, Q.-F. Zhang, B Fan, B Xue, H.-J. Chen, et al.. An extremely high rate Li–S battery with hybrid electrolyte. Journal of Alloys and Compounds, 2020, 845, pp.156261. 10.1016/j.jallcom.2020.156261 . hal-02932002

HAL Id: hal-02932002
https://hal.science/hal-02932002

Submitted on 11 Sep 2020

HAL is a multi-disciplinary open access archive for the deposit and dissemination of scientific research documents, whether they are published or not. The documents may come from teaching and research institutions in France or abroad, or from public or private research centers.

L'archive ouverte pluridisciplinaire **HAL**, est destinée au dépôt et à la diffusion de documents scientifiques de niveau recherche, publiés ou non, émanant des établissements d'enseignement et de recherche français ou étrangers, des laboratoires publics ou privés.

Journal Pre-proof

*Credit Author Statement

Yang-Hai Xu: Conceptualization, Methodology, Writing - Original Draft.

Quan-Feng Zhang, **Bai Xue** and **Hui-Jian Chen**: Validation, Investigation and Data curation.

Xiang-Hua Zhang, **Zhong-Kuan Luo**, **Fang Wang**, **David Le Coq**, **Laurent Calvez** and **Hong-Li Ma**: Formal analysis, Software, Visualization and Writing-Review & Editing.

Bo Fan and **Ping Fan**: Resources, Supervision and Funding acquisition.

Journal Pre-proof

Yang-Hai Xu[a,b], Quan-Feng Zhang[a], Bo Fan[a*], Bai Xue[a], Hui-Jian Chen[a], Xiang-Hua Zhang[a,d], Zhong-Kuan Luo[c], Fang Wang[c], David Le Coq[d], Laurent Calvez [d], Hong-Li Ma[d], Ping Fan[a*]

[a] Shenzhen Key Laboratory of Advanced Thin Films and Applications, Institute of Thin Film Physics and Applications, College of Physics and Energy, Shenzhen University, 518060 Shenzhen, China.

[b] Key Laboratory of Optoelectronic Devices and Systems of Ministry of Education and Guangdong Province, College of Optoelectronic Engineering, Shenzhen University, Shenzhen 518060, China.

[c] College of Chemistry and Environmental Engineering, Shenzhen University, 3688 Nanhai Avenue, Nanshan District, Shenzhen, 518060, China

[d] Univ. Rennes, CNRS, ISCR (Institut des Sciences Chimiques de Rennes)-UMR 6226, Rennes, FR 3504 (*corresponding author: fanb07@hotmail.com; fanping308@126.com)

Journal Pre-proof

An extremely high rate Li-S battery with hybrid electrolyte

Yang-Hai Xu[a,b], Quan-Feng Zhang[a], Bo Fan[a,z], Bai Xue[a], Hui-Jian Chen[a], Xiang-Hua Zhang[a,d], Zhong-Kuan Luo[c], Fang Wang[c], David Le Coq[d], Laurent Calvez [d], Hong-Li Ma[d], Ping Fan[a,z]

[a] Shenzhen Key Laboratory of Advanced Thin Films and Applications, Institute of Thin Film Physics and Applications, College of Physics and Energy, Shenzhen University, 518060 Shenzhen, China.
[b] Key Laboratory of Optoelectronic Devices and Systems of Ministry of Education and Guangdong Province, College of Optoelectronic Engineering, Shenzhen University, Shenzhen 518060, China.
[c] College of Chemistry and Environmental Engineering, Shenzhen University, 3688 Nanhai Avenue, Nanshan District, Shenzhen, 518060, China
[d] Univ. Rennes, CNRS, ISCR (Institut des Sciences Chimiques de Rennes)-UMR 6226, Rennes, FR 35042
([z],corresponding author: fanb07@hotmail.com; fanping308@126.com)

Key words: $Li_{10}SnP_2S_{12}$, sulfide solid electrolyte, hybrid electrolyte, Li-S battery, safety

An extremely high rate Li-S battery is obtained with hybrid electrolyte of SSE-LE.

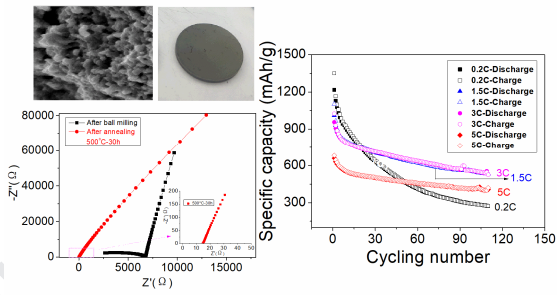

Journal Pre-proof

Journal Pre-proof

An extremely high rate Li-S battery with hybrid electrolyte

Yang-Hai Xu[a,b], Quan-Feng Zhang[a], Bo Fan[a, z], Bai Xue[a], Hui-Jian Chen[a], Xiang-Hua Zhang[a,d], Zhong-Kuan Luo[c], Fang Wang[c], David Le Coq[d], Laurent Calvez [d], Hong-Li Ma[d], Ping Fan[a, z]

[a] Shenzhen Key Laboratory of Advanced Thin Films and Applications, Institute of Thin Film Physics and Applications, College of Physics and Energy, Shenzhen University, 518060 Shenzhen, China.

[b] Key Laboratory of Optoelectronic Devices and Systems of Ministry of Education and Guangdong Province, College of Optoelectronic Engineering, Shenzhen University, Shenzhen 518060, China.

[c] College of Chemistry and Environmental Engineering, Shenzhen University, 3688 Nanhai Avenue, Nanshan District, Shenzhen, 518060, China

[d] Univ. Rennes, CNRS, ISCR (Institut des Sciences Chimiques de Rennes)-UMR 6226, Rennes, FR 35042

([z] corresponding author: fanb07@hotmail.com; fanping308@126.com)

Journal Pre-proof

Abstract

Polysulfide shuttling and lithium dendrites are two major issues which hinder the development of high-performance Li-S batteries. An ideal solution is to employ hybrid electrolyte consisting of sulfide solid electrolyte (SSE) and liquid electrolyte (LE), where SSE functions as a barrier for suppressing polysulfide shuttling and lithium dendrite growth while LE works as fast Li^+ transport media. In this work, $Li_{10}SnP_2S_{12}$ membranes, with a ceramic-like dense structure, provide a rigid barrier for preventing polysulfide shuttling and lithium dendrite growth. Meanwhile, its high ionic conductivity of 3.33×10^{-3} S/cm (25 ^{o}C), accompanied with good wetting

Journal Pre-proof

and Li^+ transport abilities of LE, renders the hybrid electrolyte system an excellent Li^+ dynamic property. Consequently, the Li-S batteries fabricated with this SSE-based hybrid electrolyte system can operate at an extremely high charge/discharge rate. At a rate of 5C (7.10 mA/cm^2), the batteries show an initial discharge capacity of 659.4 mAh/g, maintain at 471.4 mAh/g and 413.3 mAh/g after 50 and 100 cycles，showing a capacity retention of 71.53% and 62.67%, respectively. It is also proposed that a competitive mechanism exists between the electrochemical reaction and side reaction during cycling, where the electrochemical reaction dominates at high rates.

1. Introduction

Li–S battery is believed to be one of the most promising next-generation energy storage systems due to its superior high theoretical specific energy density as well as sulfur's inexpensive, nontoxic characteristics and abundance in nature [1,2]. A conventional Li–S battery is normally comprised of a lithium metal anode, an organic liquid electrolyte (LE), and a sulfur composite cathode. The overall reaction is involved with $S_8 + 16Li^+ + 16e^- \longrightarrow 8Li_2S$, obtaining an average voltage of 2.15 V and a specific capacity of 1672 mAh/g [3,4]. Despite so many potential advantages, a lot of challenges are still needed to address. First of all, the raw materials sulfur ($\sim 10^{-30}$ S/cm) and the final product lithium sulfides ($\sim 10^{-13}$ S/cm) are insulated, and the transformation during cycling leads to great volume changes (71 mol/L to 36 mol/L), resulting in unstable electrochemical contact within the sulfur electrode and therefore poor rate capability [4,5]. Secondly, the soluble polysulfide intermediates shuttle between the anode and cathode during cycling, leading to gradually increased electrode degradation, capacity fading and coulombic efficiency declining. Lastly, the poorly controlled Li/electrolyte interface can cause cell

Journal Pre-proof

deformation and even seriously destroy the cell with sharpened lithium dendrites. A very large proportion of Li−S pouch cells fail by the Li metal powdering and electrolyte depletion, which is usually induced by the uncontrolled Li dendrite growth [6].

Among all the challenges, polysulfide shuttling is one of the main reasons causing low coulombic efficiency, rapid capacity fading and poor rate capability of Li–S batteries [2, 5]. The conventional polymer separators fail to act as a selective physical barrier for polysulfides. Tremendous effort has been made to modify the cathode structure [3,7,8], tailor electrolyte [9,10] and control the electrochemical process [11,12] in order to confine polysulfides in the cathode, however with limited success. Polysulfide shuttling and capacity fading could be temporarily suppressed but not be thoroughly avoided.

An alternative solution to polysulfide shuttling is to replace the conventional organic liquid electrolytes (LE) by polymer electrolytes [13] or dense inorganic solid electrolytes [14,15]. However, poor ionic conductivity at room temperature and non-intimate interfacial contact between electrolyte and electrode materials induce large internal resistance of solid-state Li-S batteries, and therefore limit their performance under high charge/discharge rate [16,17]. A possible way is to implant hybrid electrolyte to Li-S batteries, with inorganic solid electrolyte being used as polysulfide barrier while organic electrolyte [18,19], ionic liquid electrolyte [20,21] or gel-polymers [22,23] used as wetting agent to improve interfacial contact and as high speed bridge for fast Li^+ transportation [24,25]. Among these hybrid electrolytes referred above, oxide electrolytes, such as LAGP ($Li_{1.5}Al_{0.5}Ge_{1.5}(PO_4)_3$), LATP ($Li_{1.3}Al_{0.3}Ti_{1.7}(PO_4)_3$), etc., are usually used as the inorganic barrier. However, the ionic conductivity of oxide electrolytes is still not high enough to satisfy the high-rate operation of the batteries. Furthermore, it necessitates high

Journal Pre-proof

temperature for calcination. Sulfide solid electrolytes (SSE), such as, $Li_{10}GeP_2S_{12}$ [26], $Li_7P_3S_{11}$ [27], $Li_{10}SnP_2S_{12}$ [28] and $Li_{9.54}Si_{1.74}P_{1.44}S_{11.7}Cl_{0.3}$ [29], is more attractive than oxides due to its ionic conductivity higher than 5×10^{-3} S/cm and feasible deformability at ambient temperature, in spite of its undesirable sensitivity to moisture. Therefore, in comparison with oxide-liquid hybrid electrolytes, the combination of SSE and organic liquid electrolyte (SSE-LE) is more promising to construct a hybrid electrolyte system which enables the batteries operate at high rate.

In this work, a Li-S battery is fabricated with hybrid electrolyte consisting of a highly ionic conductive sulfide solid electrolyte ($Li_{10}SnP_2S_{12}$, with ionic conductivity of 3.33×10^{-3} S/cm) and liquid electrolyte (LE, 1M LiTFSI DME/ DOL(50-50, v %)+1% $LiNO_3$), pre-soaked Li metal anode and S-C composite cathode, exhibiting a superior high rate capability. At a high charge/discharge rate of 5C (12.532 mA or 7.10 mA/cm^2), the Li-S battery with hybrid electrolyte shows an initial discharge capacity of 659.4 mAh/g, maintaining at 471.4 mAh/g and 413.3 mAh/g after 50 and 100 cycles with the capacity retention of 71.53% and 62.67%, respectively. The sulfide solid electrolyte, $Li_{10}SnP_2S_{12}$, is chosen as inorganic solid electrolyte here due to its cheap price, natural abundance of raw materials, and especially the high ionic conductivity. Moreover, a robust structure of the $Li_{10}SnP_2S_{12}$ membranes obtained after 500 ^oC annealing ensures the batteries free of polysulfides shuttle and lithium dendrite penetration, making it more competitive than other highly ionic conductive SSE, such as Li_2S-P_2S_5. The electrochemical process and structure/ morphology change of the SSE-based hybrid Li-S battery are also detailly investigated.

2. Experimental

2.1 Materials synthesis and characterization

Journal Pre-proof

Stoichiometric Li_2S, S, Sn and P_2S_5 (Sigma-Aldrich, ≥99.99%) were loaded in a tungsten carbide jar and mechanically alloyed under argon atmosphere(O_2＜0.5 ppm, H_2O＜0.5 ppm) by using 8000D Mixer/Miller at 875 rpm for 60 h for the preparation of $Li_{10}SnP_2S_{12}$ compound. The ball-milling process was intermittently paused and the reactants were manually mixed every 10 h for homogeneity. The ball-milled powder was then sieved by a 500-mesh sieve and cold-pressed into pellets with to diameter of 15 mm and thickness of 0.85 mm under a pressure of 320 MPa. The SSE was finally obtained by annealing the above pellets at 500 ^oC for 30 h in sealed silica tube with a vacuum level higher than 10^{-3} Pa. S-C composite was prepared by heating a well-ground mixture of S and ketjen black at 155 ^oC for 20 h in a sealed silica tube [3] from which sulfur could distribute homogeneously inside the micro- and meso-pores of ketjen black via capillary action (see ESI, Figure S1).

The morphology of the samples was characterized by using a JEOL JED2300 thermal field emission scanning electron microscopy (SEM) operating at 2.0 kV, and its energy dispersive X-Ray spectroscopy (EDS) accessory was used for element analysis. Thermogravimetric analysis (TGA) was performed to study the S content in the S-C composite, with N_2 as a flow gas and a ramp rate of 10 ^oC/min. The accurate sulfur content was determined to be 57.17% by TGA (see ESI, Figure S2). The phase structure of the SSE was analyzed by using a Panalytical Empyrean multipurpose X-ray diffractometer (XRD) with a Cu Kα (1.5406 Å) radiation in the diffraction angle range of 10°– 90°. Raman spectroscopy was performed on inVia confocal Raman microscope ((Renishaw)) with a 532-nm diode-pumped solid-state laser and a grating of 1800 lines/mm. In order to protect the SSE against ambient moisture, samples were covered by a transparent kapton tape during XRD and Raman measurements.

Journal Pre-proof

2.2 Electrochemical performance measurements

Ionic conductivity of the SSEs was obeyed Arrhenius law: $\sigma_{dc}T = A \exp(-E_A/k_BT)$. It was measured by AC impedance method on a Solartron 1260A frequency response analyzer. For this measurement, the SSE powders were cold-pressed into pellets (15 mm diameter and ~0.7 mm thickness) under 350 MPa pressure, with carbon paint on both sides as inert electrodes. Conductivity was calculated by equation $\sigma = L/(RS)$, where L, R and S represent thickness, resistance and electrode area of samples, respectively.

The Li stripping/plating behaviour was studied on symmetric cells with a structure of Li/LE/SSE/LE/Li, and the test was conducted by using a Wuhan Land CT2001 battery tester. The symmetric cell was assembled by stacking a Li foil, an SSE pellet and another Li foil into a Swagelok battery mould, with 10 μL ether-based LE dropped between the SE pellet and the Li electrodes.

A Li-S battery with hybrid electrolyte was assembled in a Ar-filled glove-box (O_2＜0.5 ppm, H_2O＜0.5 ppm) with a sandwich structure of –)SUS/ Li/ LE-SSE-LE (liquid electrolyte, 1M LiTFSI DME/Dol-1%$LiNO_3$)/ S/ SUS(+. Lithium foil was pre-soaked in LE for 3 days, and dried naturally until its surface showed a gel state before being used as the anode. The pretreatment is helpful to form a SEI layer mainly composed of LiF [6,30]on Li surface, which can alleviate the interfacial incompatibility between $Li_{10}SnP_2S_{12}$ and Li [31]. Meanwhile, it can also improve the contact between them. The cathode was obtained by ultrasonic spraying an alcoholic suspension of S-C composite, LA133 binder and acetylene black (80:10:10, w %) on carbon paper. The cathode was wetted by transient dip into LE before use. 10 μL LE was additionally dropped on each side of the SSE membrane and the SSE membrane was then covered by the anode and the

Journal Pre-proof

cathode to form the sandwich structure. Finally, the batteries were packaged into CR2032-type coin cells. The batteries were stored in glove-box one night before test.

For comparison, Li-S batteries with only LE or SSE ($Li_{10}SnP_2S_{12}$ compound) were also assembled. For the liquid-electrolyte battery, the assemble procedure is the same as the hybrid-electrolyte battery, except that the SSE membrane was replaced by LE-wetted Celgard® 2400 membrane. For the all-solid-state battery, the composite cathode was firstly prepared by ball-milling a mixture of sulfur, ketjen black and SSE (25:25:50, w.%) at 450 rpm for 6 h. The composite cathode were then cold pressed on one side of SSE under 300 MPa. Li foil was put on the other side of SSE. Finally the Li/ SSE/ S-C structure was loaded in a homemade cell mould for battery test. The galvanostatic charge-discharge test was carried out on a Wuhan Land CT2001 battery tester with different charge/discharge rate. The cut-off voltages were set at 1.5 V and 2.8 V. Cyclic voltammetry (CV) was performed to investigate the redox reaction of the Li-S batteries at a scanning rate of 0.1 mV/s between 1.4 V and 3.0 V.

Journal Pre-proof

3. Results and discussion

3.1 Materials evaluation

In this study, $Li_{10}SnP_2S_{12}$ is synthesized by high energy ball milling plus post annealing. This synthesis route is different from the one reported in previous study [28], where a long-term solid-state reaction (> 216 h) under a high temperature (> 600 ^{o}C) was carried out for the synthesis. By using our new method, both the time and power for synthesis can be greatly saved, making it a promising large-scale synthesis route of $Li_{10}SnP_2S_{12}$.

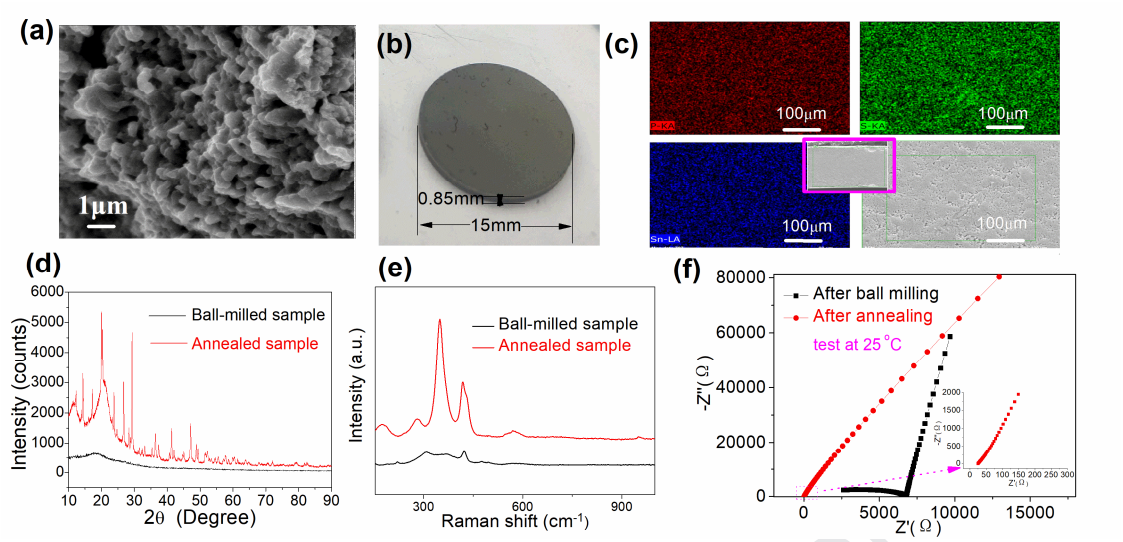

Figure 1. Material characterizations of the SSE samples. (a) SEM image of the $Li_{10}SnP_2S_{12}$ powder; (b) photograph of the $Li_{10}SnP_2S_{12}$ membrane (φ15 mm × 0.85 mm); (c) EDS mapping of the $Li_{10}SnP_2S_{12}$ membrane, and the inset shows the SEM image of its cross-section; (d) XRD patterns, (e) Raman spectra and (f) AC impedance spectra of the SSE samples before and after annealing.

Figure 1 presents the material characterization results of the $Li_{10}SnP_2S_{12}$ (SSE) samples. Typical morphology of the as-annealed $Li_{10}SnP_2S_{12}$ powder is shown in Figure 1 and Figure S3. The particles are interconnected/agglomerated in clusters with diameter of several hundred nanometers in the powder. For the as-milled and the as-annealed $Li_{10}SnP_2S_{12}$ (see Table S1) powders, S/Sn and P/Sn mole ratios are 11.82, 2.01 and 11.55, 1.97, respectively, which is not so perfectly consistent with but very close to the stoichiometry S/Sn=12, P/Sn=2. As shown in Figure 1b and 1c, it can be observed that the SSE membrane has a very dense and smooth surface with no visible cracks or pores. Such a robust structure is associated with the inter-connected nano-sized morphology of the green powder which improves the sintering performance. EDS mapping (Figure 1c) shows that all the elements, S, Sn and P, are homogeneously distributed in the SSE membrane. This robust structure is similar to the high-temperature-sintered dense ceramics.

Journal Pre-proof

Remarkably, such a dense structure is rarely found in other SSEs, for example, Li_2S-P_2S_5 system [27], due to their relatively low sintering temperature (230–260 ^oC) which is necessary to avoid undesired decomposition. Thus, $Li_{10}SnP_2S_{12}$ membrane can be used as both electrolyte for fast ion transport and robust physical barrier for the suppression of polysulfides shuttling and lithium dendrite penetration, in all-solid-state and hybrid-electrolyte Li-S batteries.

Figure 1d shows X-ray diffraction patterns of as-milled and as-annealed $Li_{10}SnP_2S_{12}$ samples. The broad diffraction peak around 18^o is attributed to a kapton tape cover on the samples. The powder synthesized after ball milling is typically amorphous since no diffraction peaks are identified from the XRD pattern. After annealing, the intense diffraction peaks attributed to $Li_{10}SnP_2S_{12}$ can be obviously identified [27], indicating that well-crystallized $Li_{10}SnP_2S_{12}$ is obtained. Figure 1e shows the Raman spectra of the SSE ($Li_{10}SnP_2S_{12}$) membrane before and after annealing. The peaks below 200 cm^{-1} are attributed to poor bonded Li^+. Its broad profile is consistent with the structure disorder of lithium sub-lattice. The peak at 276 cm^{-1} is probably due to PS_4 tetrahedra. The most intense peak around 351 cm^{-1} is attributed to SnS_4 tetrahedra. The presence of two overlapped intense peaks around 420 cm^{-1} is possibly originated from two different structural sites of PS_4 tetrahedra. The Raman result is in accordance with that reported by P. Bron [28] who collects information from the Raman spectra of Li_4SnS_4 and Li_3PS_4.

The AC impedance spectra of the SSE samples show typical ionic conductivity behavior with a tail at low frequency and a semicircle at high frequency (disappears in the as-annealed sample due to its high ionic conductivity), as seen in Figure 1f. The as-milled SSE sample shows a low ionic conductivity of 7.39×10^{-6} S/cm, which is greatly enhanced by about 3 orders of magnitude to 3.33×10^{-3} S/cm after annealing at 500^oC for 30 h. This high ionic conductivity of SSE can be

Journal Pre-proof

attributed to its similar structure to the super-ionic conductor $Li_{10}GeP_2S_{12}$, with a one-dimensional (1D) lithium conduction pathway along the c axis [28]. Li^+ can freely move through the crystal lattice via direct jumps between the partially occupied positions rather than unoccupied interstitial sites. The SSE with extremely high ionic conductivity is promising for fabricating Li-S batteries with high rate capability.

3.2 Battery performance

Li–S batteries with hybrid electrolyte are fabricated here with S-C composite cathode (with S load of 0.85 mg/cm^2, Figure S1 and Figure S2), LE-SSE hybrid electrolyte, and Li foil anode. The Li foil was soaked in LE for three days before use. This process helps to form a protective SEI film (mainly composed of LiF) on the surface of Li foil [6,31]. An average open circuit voltage of about 2.36 V is observed on the as-assembled batteries. Figure 2 shows the galvanostatic discharge/charge profiles of the Li–S batteries with hybrid electrolyte at different rates (1 C = 1675 mA g^{-1} or 2.5 mA or 1.42 mA/cm^2). All the profiles share the same features with the liquid-electrolyte batteries, that is, consist of two distinct discharge plateaus and two overlapped charge plateaus. These stepwise discharge and charge profiles are the consequence of a two-step conversion between S_8 and Li_2S/Li_2S_2 via the formation of intermediate lithium polysulfides [1,2]. Therefore, the Li-S batteries with hybrid electrolyte and with liquid electrolyte have the same reaction mechanism within the electrodes. In fact, in hybrid-electrolyte batteries, the electrode materials are still under liquid-electrolyte environment, while the solid electrolyte membrane only acts as a barrier and an ion-conductor between the electrodes but does not participate in the electrochemical reaction (Figure 2d). The initial capacity of the first plateau is relatively independent on the discharge rate (close to 300 mAh/g, see Figure 2c), while the capacity of the

second plateau decreases with increasing discharge rate [32].

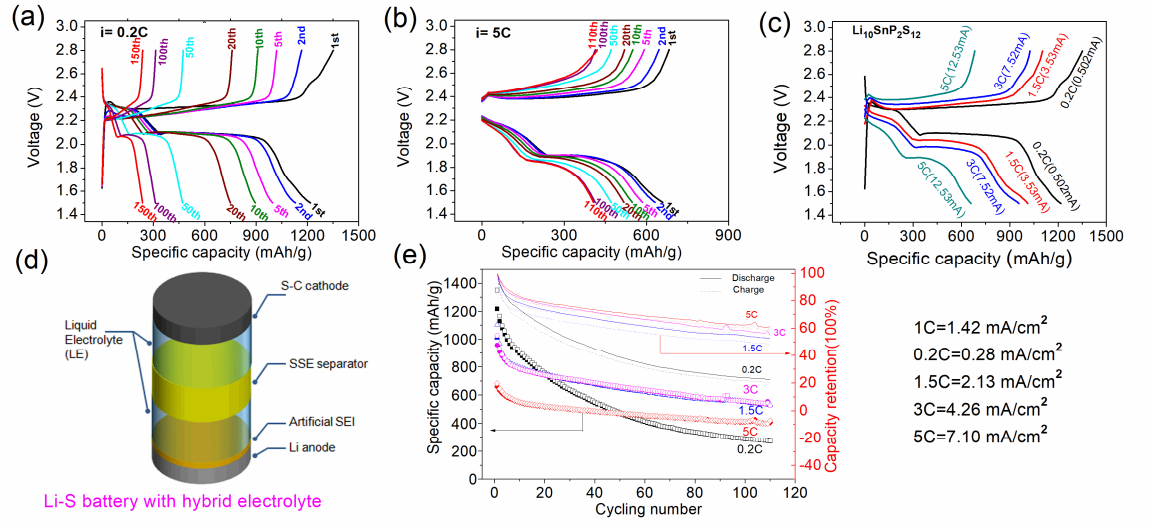

Figure 2. Electrochemical performances of the Li-S batteries with hybrid electrolyte. (a-b) Galvanostatic charge-discharge profiles at a charge/discharge rate of 0.2C and 5C; (c) Initial cycling performance at different charge/discharge rates; (d) Scheme of the Li-S battery with hybrid electrolyte; (e) Cycle performance and capacity retention at different charge/discharge rates.

At a low charge/discharge rate of 0.2C, the Li-S battery with hybrid electrolyte exhibits an initial discharge capacity of 1217.3 mAh/g and charge capacity of 1350.9 mAh/g. The discharge plateau (2^{nd}) is of 2.10 V and the charge plateau is of 2.28 V, resulting in a quite small overpotential ΔV = 0.18 V. After 50 cycles, the capacity decreases to 471.2 mA h/g for discharge and 474.4 mA h/g for charge. This fast decaying of capacity is possibly related with side reactions between SSE and electrodes or LE, which lead to continuous loss of active materials. This point will be detailly discussed later. For 1.5C, 3C and 5C, the Li-S batteries with hybrid electrolyte exhibit an initial discharge capacity of 1011.3 mAh/g, 956.9 mAh/g, 659.4 mAh/g and charge capacity of 1103.3 mAh/g, 1025.3 mAh/g and 682.7 mAh/g, respectively (see Figure 2b,e, Figure S4). The corresponding discharge plateau (2^{nd}) and charge plateau are of 2.04 V, 1.98 V, 1.89 V

Journal Pre-proof

and of 2.32 V, 2.35 V, 2.40 V, respectively (△V=0.28 V, 0.37 V and 0.51 V, Table S2). Both discharge voltage and capacity of the studied batteries are superior to those of hybrid Li-S batteries composed by oxide solid electrolyte such as LAGP [22, 23], which is possibly related with the higher ionic conductivity of SSEs. It's obvious that a higher charge/discharge rate can cause a lower capacity and a higher overpotential. It is possibly due to a larger cathode polarization caused by a high coverage of the insulated Li_2S particles on the carbon skeleton when the batteries operate at a high rate [32].

As shown in Figure 2e and Figure S4，at a charge/discharge rate of 1.5C and 3C, the battery capacity decreases slowly during cycling, maintaining a level higher than 540 mAh/g after 100 cycles with the capacity retention respectively of 54.51% and 58.05%. Especially, at a higher rate of 5C, the Li-S battery with hybrid electrolyte shows an initial discharge capacity of 659.4 mAh/g, maintaining at 471.4 mAh/g and 413.3 mAh/g for both discharge and charge process after 50 and 100 cycles with the capacity retention of 71.53% and 62.67%, respectively. Besides, the batteries keep a high second discharge plateau more than 1.89 V even after 100 cycles under 5C operation. This is the first report on hybrid-electrolyte Li-S batteries which can successfully run more than 100 cycles at an extremely high rate of 5C. Such an excellent rate capability makes the hybrid-electrolyte Li-S batteries with $Li_{10}SnP_2S_{12}$ membrane very competitive compared to previously reported liquid-electrolyte Li-S batteries [33,34] and hybrid-electrolyte Li-S batteries with oxide electrolyte membrane [23, 24].

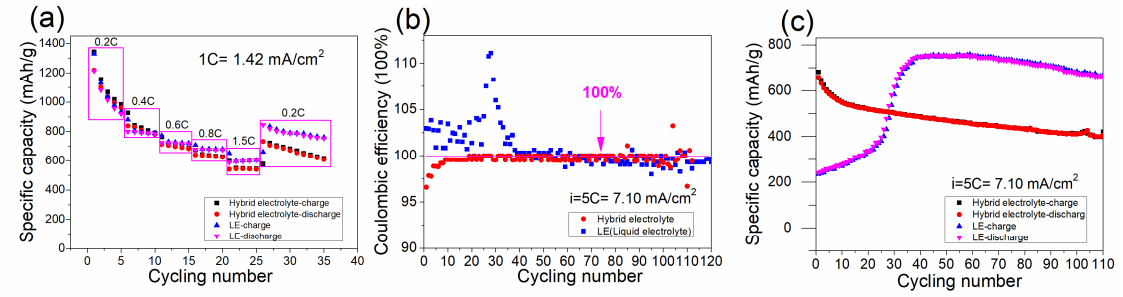

Figure 3. Comparison of the battery performance between the SSE-based hybrid-electrolyte batteries and the liquid-electrolyte batteries. (a) Rate capability, (b) Coulombic efficiency and (c) Cycling performance of the two kinds of batteries.

Here the performance of Li-S batteries with three different electrolytes, hybrid electrolyte, liquid electrolyte and solid electrolyte, is compared. As shown in Figure 3, both the Li-S batteries with hybrid electrolyte and liquid electrolyte can stably operate at a high rate. For both the hybrid-electrolyte and liquid electrolyte Li-S batteries, they possess an initial voltage of 2.40 V and a voltage plateau of 2.10 V f at 0.2C during discharge (Figure S5). Differently, the all-solid-state Li-S battery can only operate at a very low rate of 0.15C due to its high electrode/electrolyte interfacial resistance. Moreover, its capacity decreases fast, which is associated with the fast-growing interfacial resistance after cycling (see Figure S6 and Figure S7). Compared with the liquid-electrolyte batteries, the hybrid-electrolyte batteries exhibit somehow lower capacity. It is ascribed to the active material loss by side reactions that will be detailly discussed later. However, the capacity of the hybrid-electrolyte batteries is much higher than that of the all-solid-state batteries, which is benefited from the improved electrolyte/electrode contact by wetting the electrode materials with liquid electrolyte [18-20, 35].

Despite of the slightly lower capacity, the hybrid-electrolyte batteries exhibit higher coulombic efficiency and better activating performance than the liquid-electrolyte batteries. As

Journal Pre-proof

shown by Figure 3b, the coulombic efficiency of the hybrid-electrolyte batteries is stable at about 100%, while the coulombic efficiency of the liquid-electrolyte batteries gradually decreases to lower than 100% after about 40 activating cycles. The coulombic efficiency approaching 100% implies that polysulfide shuttling is thoroughly suppressed in the hybrid-electrolyte batteries, proving that the $Li_{10}SnP_2S_{12}$ membrane acts as a perfect physical barrier for the polysulfide intermediates. Moreover, the liquid-electrolyte batteries exhibit an activating process when operating at high rate, which is reflected by the gradual increase of capacity during the initial cycles (Figure 3c and Figure S5) [36]. This activating process is absent in the hybrid-electrolyte batteries, showing their better activating performance.

Table 1. Electrochemical performance of the SSE-based hybrid-electrolyte batteries, in comparison with other reported hybrid-electrolyte batteries and liquid-electrolyte batteries.

Electrolyte	**σ_{SE} (mS/cm)**	**Rate**	**Capacity (mAh/g)**		**Discharge plateau (V)**		**Reference**
			1st cycle	50th cycle	1st cycle	50th cycle	
SSE-LE	3.3	0.2C	1217	471	2.10	2.10	Our work
		5.0C	659	471*	1.92	1.83	Our work
LAGP-LE	0.18	0.2C	1386#	/	2.08#	/	[37]
LAGP-FDE	0.32	0.1C	1478	915	1.95	1.75	[18]
		1.0C	915	668	1.0	/	[18]
LATP-LE	/	0.2C	1100	830	2.04	1.92	[23]
LATP -LE	/	0.1C	978	750	2.03	2.02	[38]
LE	/	0.2C	1409	919	2.10	/	[36]
		5.0C	602	565*	1.88	1.95	[36]

* represents after 100th cycling. # represents after 40th cycling.

Table 1 lists some performance parameters of the studied hybrid-electrolyte batteries with $Li_{10}SnP_2S_{12}$ membrane, in comparison with other reported hybrid-electrolyte (oxides) batteries and liquid electrolyte batteries. As shown in Table 1, most of the reported hybrid electrolytes use oxide membranes (LAGP [18, 37], LATP [23, 38]), which show a low ionic conductivity of about 10^{-4}

Journal Pre-proof

S/cm and therefore lead to low rate capability. The oxide-LE hybrid system exhibits a low discharge voltage plateau even when running at only 1C [18]. The hybrid-electrolyte Li-S batteries with $Li_{10}SnP_2S_{12}$ membrane are comparable to LE system when referred to the rate performance, exhibiting a high capacity and high discharge voltage plateau at a high rate of 5C. Moreover, there's no activation process and the coulombic efficiency is stably high. The only drawback is the capacity loss induced by the instability between the $Li_{10}SnP_2S_{12}$ membrane and the electrodes or LE, which can be avoided by advanced interfacial modification techniques [39]. As a result, SSE-LE hybrid electrolyte system is a promising candidate for fabricating high rate Li-S batteries.

3.3 Stability and failure analysis of the batteries

To understand the redox reactions that occur in the Li-S batteries with hybrid electrolyte, CV tests of the batteries are conducted at a scan rate of 0.1 mV/s from 1.4 V to 3.0 V and the CV curves are presented in Figure 4a. A Li-S battery with LE is also fabricated here to make a comparison. Similar to the Li-S battery with LE, there are two visible cathodic current peaks positioned at 2.30 V and 2.05 V for the hybrid system, corresponding to the conversion of cathode materials from sulfur to high-order polysulfides (Li_2S_n , $4\leq n<8$) and from high-order polysulfides to low-order polysulfides (Li_2S_n , $n<4$) and finally to insoluble lithium sulfide (Li_2S_2 /Li_2S) , respectively. There're two anodic current peaks positioned at 2.40 V and 2.50 V which belong to the conversion of low-order polysulfides back to high-order polysulfides and then to S_8^{2-}/S_8 [1,2]. It is worth noting that the position of the redox current peaks in the hybrid-electrolyte battery is almost the same as the liquid-electrolyte one, which is good evidence to demonstrate the excellent redox dynamics with the hybrid electrolyte system.

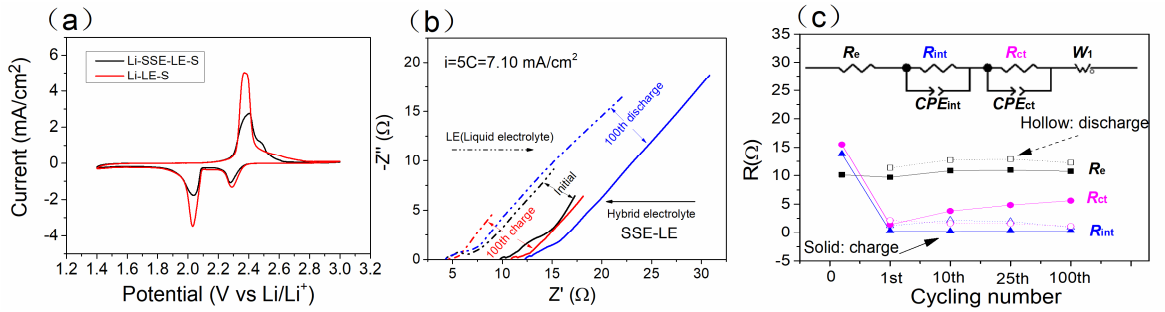

Figure 4. Electrochemical characterization of the Li-S batteries with hybrid electrolyte and liquid electrolyte. (a) CV curves of batteries between 1.4 V and 3.0 V; (b) Impedance spectra of batteries after fully charging to 2.8 V, or discharging to 1.5 V at a current density of 5C (7.10 mA/cm^2); (c) Evolution of the bulk resistance *Re*, the interfacial resistance R_{int} and the charge transfer resistance R_{ct} deduced from the impedance spectra with equivalent circuit shown in the inset.

The AC impedance spectra of the batteries, as can be seen in Figure 4b and Figure S8-10, are typically composed of two semi-circles and a tail, which correspond to the interfacial resistance, the charge transfer resistance and the lithium ion diffusion at the electrode, respectively [23,40]. In the virginal batteries, the total resistances for the Li-S batteries with LE and hybrid electrolyte are about 50 Ω and 40 Ω, respectively. The resistances quickly decreases to about 10 Ω for the liquid-electrolyte batteries and 20 Ω for the hybrid-electrolyte batteries after the first charge/discharge cycle and maintain at this level for the whole cycling process (see Figure 4b, Figure S8 and Figure S9). Both the two types of Li-S batteries exhibit a low internal resistance, thus promising for fabricating high rate Li-S batteries, which has already been demonstrated by their stable operation at 5C rate (see Figure 3c).

With the equivalent circuit depicted in Figure 4c, the bulk resistance R_e, the interfacial resistance R_{int} and the charge transfer resistance R_{ct} of the hybrid-electrolyte batteries can be determined by fitting the AC spectra (Figure S10). The detailed evolution of these resistances is

Journal Pre-proof

plotted in Figure 4c. It's obvious that there's a positive shift (from 10 Ω to 11 Ω for charge, and 12 Ω to 13 Ω for discharge, Figure S9) of the bulk resistance R_e after the 1st cycle, which is possibly a reflection of an irreversible local structure change of the batteries. As discharge proceeds, sulfur transforms to soluble polysulfides, and thus the viscosity of electrolyte increases, resulting in an increase of the electrolyte resistance. This could be another origin of the increased R_e (from about 10 Ω to 11 Ω for 1^{st} cycle, and 11 Ω to 13 Ω for 2^{nd}, 10^{th}, 25^{th} and 100^{th} cycle, Table S3). It's highlighted that there's almost no change of the interfacial resistance R_{int} after the 1^{st} cycle (Figure S11), indicating that stable interfaces between SSE membrane and electrodes have been formed. The charge transfer resistance R_{ct} somehow increases during the charge/discharge cycling (see Figure 4c and Figure S11), which might be ascribed to the formation and decomposition of insulated volume-expanded Li_2S particles, causing slower mass and electron dynamics. Notably, even after 100 cycles, the Li-S battery with hybrid electrolyte still shows a very small total resistance, enabling a long-term high rate operation of the battery.

Remarkably, such a low internal resistance revealed in our SSE-based hybrid-electrolyte Li-S batteries is one or two orders of magnitude lower than that of the previously reported hybrid-electrolyte Li-S batteries with oxide electrolyte membrane [18,23,24]. This low internal resistance, which is an essential prerequisite for high rate operation of the batteries, is of course benefited from the high ion-conduction ability of the $Li_{10}SnP_2S_{12}$ SSE membrane as well as the improved interfacial contact between SSE and electrodes.

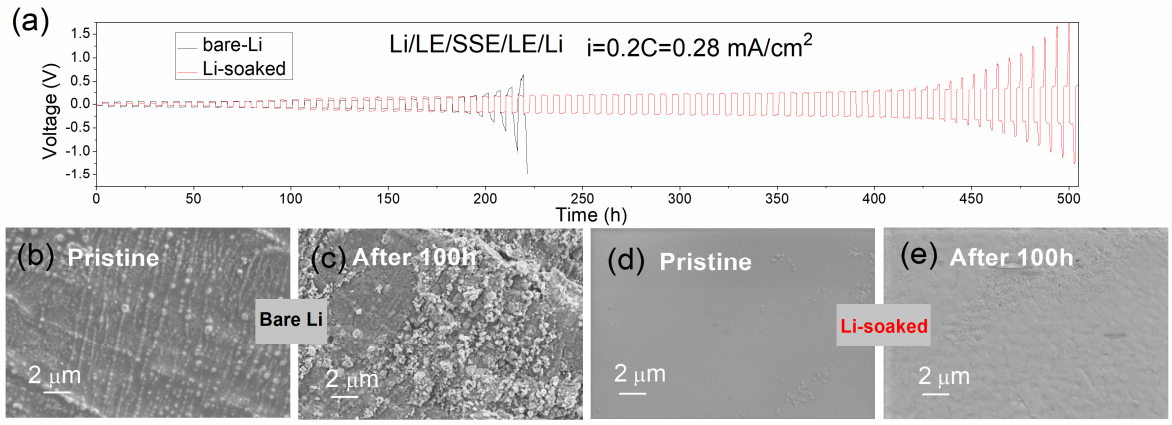

Figure 5. Li plating/stripping behavior of Li symmetric cells and corresponding morphology change of Li foil surface before and after 100 h cycling. (a) Voltage versus time for the Li symmetric cells where each half-cycle lasts 3 h at a current density of 0.28 mA/cm^2; (b-e) Morphology changes of the surface of bare Li and Li-soaked before and after 100 h cycling .

As shown in Figure 5a, Li symmetric cells exhibit a gradually increasing voltage for the case of both bare Li and Li-soaked, reflecting an unstable interface between SSE and Li under electrochemical environment. However, the Li-soaked cell exhibits a longer life span (450 h vs. 200 h) and slower voltage increase, demonstrating a better interfacial stability. It is observed that a very smooth SEI layer is formed on Li foil after 3-day soaking in LE, as shown in Figure 5d, which is mainly constituted of LiF as previously reported by M. Barghamadi et al. [6,30]. This SEI layer can be a good barrier for suppressing the side reaction between LSPS and Li anode. Obviously, after 100 h of Li plating/stripping, the Li foil soaked in LE displays a smooth surface except some nucleus of Li dendrites. In contrast, for the bare Li a lot of sharp Li dendrites appear on the surface (Figure 5c, Figure S12). Meanwhile, the formed SEI layer can greatly reduce the total resistance of the Li symmetric cell, and the charge transfer resistance turns out to be the dominant part during Li plating/stripping as shown by the impedance spectra of the cells in Figure S13. Therefore, it's reasonable that the hybrid Li-S batteries with Li-soaked anode exhibit an

improved cycling performance.

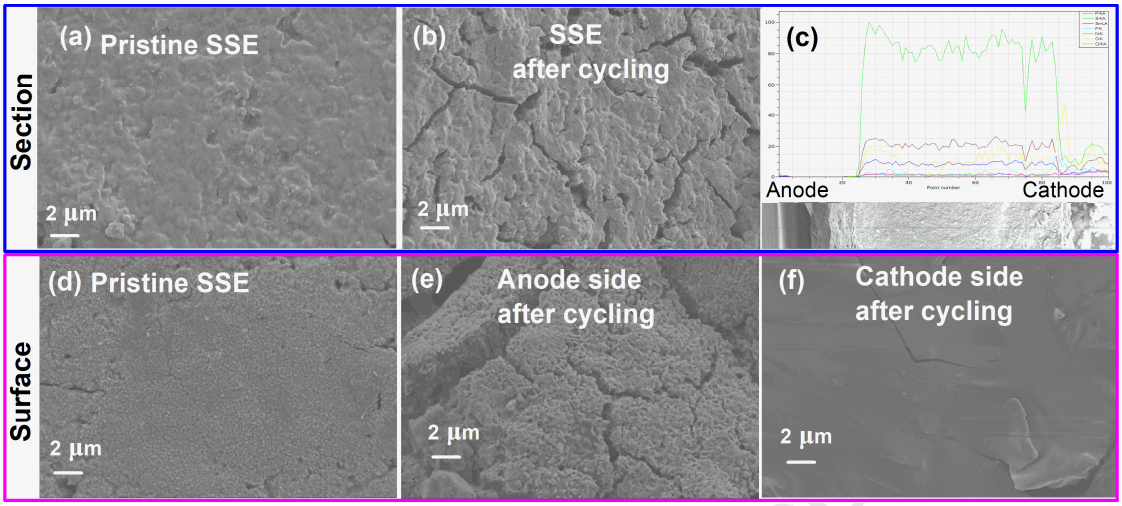

Figure 6. SEM images of the surface and cross section of SSE before (a,d) and after 100th (b,c,e,f) battery cycling. Blue zone and pink zone represent the section and surface of SSE ($Li_{10}SnP_2S_{12}$) membrane, respectively.

Figure 6 shows the morphology change of the SSE membrane before and after battery test. Apparently, the SSE membrane displays a very robust structure without any visible cracks or before battery test, as shown by the top-view and cross-sectional SEM image (Figure 6a,d). Even though some cracks generate when discharge/charge process continues, the penetration of the species in the liquid electrolyte is still kept at an extremely low level, which is indicated by the low fluorine content along the cross-section of the SSE membrane (Figure 6c, Figure S14 and Table S4), considering that fluorine is a unique elemental signal of the liquid electrolyte which is originated from the salt LiTFSI.

After 100 cycles, it shows obvious morphology change on both sides of the SSE membrane (Figure 6(e, f)). On the side face to lithium anode, a rough surface with a few huge cracks is formed, as a result of the etching of $Li_{10}SnP_2S_{12}$ under low potential versus Li^+/Li.[41,42,43]. Fortunately, the existence of liquid electrolyte between SSE membrane and Li ameliorates this

Journal Pre-proof

interfacial degradation as discussed above. On the other side face to cathode, a plain thick layer rich of S and F but deficient of Sn and P (see Table S4) is observed which probably comes from the side reaction between $Li_{10}SnP_2S_{12}$ and the intermediate polysulfides in LE. It has been reported that the nucleophilicity [44] of polysulfide makes it reactive when contacting with the elements in high valence state, such as Ti^{3+} in (NASICON)-type solid electrolyte $Li_{1+x}Ti_{2-x}Al_x(PO_4)_3$ [38]. Since $Li_{10}SnP_2S_{12}$ contains quadrivalent Sn^{4+}, a side reaction may also occur between the $Li_{10}SnP_2S_{12}$ membrane and the polysulfides, resulting in the S-rich thick layer on the cathode side of SSE membrane. It is worth noting that the S-rich layer formed on SSE is thick (Figure 6f) so it grows continuously during the cycling process which may cause an uninterrupted consumption of intermediate polysulfides and therefore the gradual capacity decay, as shown by the charge-discharge curves in Figure 2. This existence of the unwanted side reaction can be further verified by observing a non-negligible self-discharge phenomenon in a 1-week-stored hybrid-electrolyte Li-S battery (see Figure S15 and Figure S16), that is, the stored battery exhibits evidently lower capacity than the freshly assembled battery, whose initial discharge and charge capacities at 0.2C rate decrease to 964.1 mA h/g and 1063.3 mA h/g, respectively.

The coexistence of the principal electrochemical reaction of the battery and the side reaction triggers a competitive mechanism, that is, when the batteries operate at a low rate, the principal electrochemical reaction is speed-limited so that the side reaction dominates, resulting in severe active material loss, and when operate at a high rate, the principal electrochemical reaction prevails over the side reaction and therefore the loss of active materials is ameliorated. This is the reason why high capacity retention can be achieved in the batteries operating at 5.0C as shown in

Journal Pre-proof

Figure 2.

The side reaction is related with the poor chemical stability of SSE, which could be improved by interfacial engineering of the SSEs [41, 42]. A novel approach for preparation of thin protective layer is under research in our laboratory to deal with the stability issues of SSEs and the development of high rate hybrid Li-S batteries with improved cycling performance is expected.

4. Conclusions

By using a ball-milling plus vacuum-annealing technique, $Li_{10}SnP_2S_{12}$ membranes with a ceramic-like dense structure and a high room temperature ionic conductivity of 3.33×10^{-3} S/cm have been synthesized. A hybrid electrolyte system composed of the $Li_{10}SnP_2S_{12}$ membrane and an ether-based liquid electrolyte is used to fabricate high rate Li-S batteries free of polysulfide shuttling and lithium dendrites penetration. The result hybrid-electrolyte batteries show an initial discharge capacity of 659.4 mAh/g at 5C, maintaining at 471.4 mAh/g and 413.3 mAh/g for both discharge and charge process after 50 cycles and 100 cycles with the capacity retention of 71.53% and 62.67%, respectively. The excellent rate capability of Li-S battery with hybrid electrolyte is believed to be originated from the robust ceramic-like structure and high ionic conductivity of the $Li_{10}SnP_2S_{12}$ membrane, as well as its good interfacial contact with electrodes. It is proposed that a competitive mechanism exists between the battery electrochemical reaction and side reaction, where electrochemical reaction dominates at high rates. Consequently, the batteries achieve higher capacity retention under high rate operation. The side reaction is associated with the poor interfacial stability of $Li_{10}SnP_2S_{12}$ with the cathode as well as with the anode. The study on interfacial engineering techniques is being undertaken to solve this side reaction issue and high

rate hybrid Li-S batteries with improved cycling performance is expected.

.

Supporting Information

Electronic Supplementary Information (ESI) is available: SEM, EDX, XRD, TGA, the galvanostatic charge-discharge profiles. See DOI: 10.1039/x0xx00000x.

Conflicts of interest

The authors declare that there are no conflicts of interest.

Acknowledgements

The authors are grateful for funding from the National Science Foundation of China (NFSC) project (No. 61504085, No. 51702216), the Natural Science Foundation of Guangdong Province (No. 2017A030313325), the Shenzhen Key Lab Fund (ZDSYS20170228105421966), the Natural Science Foundation of Shenzhen University (No. 827-000125/827-000089) and support from Postdoctoral Science Foundation of China.

References

[1] P. G. Bruce, S. A. Freunberger, L. J. Hardwick and J. M. Tarascon, Li-O_2 and Li-S batteries with high energy storage, Nat. Mater., 11(2012) 19–29.

[2] A. Manthiram, Y. Fu, S. H. Chung, C. Zu and Y. S. Su, Rechargeable Lithium–Sulfur Batteries, Chem. Rev., 114 (2014) 11751–11787.

[3] X. L. Ji, K. T. Lee and L. F. Nazar, A highly ordered nanostructured carbon-sulphur cathode for lithium-sulphur batteries, Nat. Mater., 8 (2009) 500–506.

[4] X. Ji and L. F. Nazar, Advances in Li–S batteries, J. Mater. Chem., 20(2010), 9821–9826.

[5] S.-E. Cheon, K.-S. Ko, J.-H. Cho, S.-W. Kim, E.-Y. Chin, and H.-T. Kim, Rechargeable Lithium Sulfur Battery, J. Electrochem. Soc., 150 (2003) A800–A805.

Journal Pre-proof

Journal Pre-proof

[6] X.-B. Cheng, J.-Q. Huang, and Q. Zhang, Review—Li Metal Anode in Working Lithium-Sulfur Batteries, J. Electrochem. Soc., 165 (1) (2018) A6058-A6072.

[7] G. Zheng, Q. Zhang, J. J. Cha, Y. Yang, W. Li, Z. W. Seh, and Y. Cui, Amphiphilic surface modification of hollow carbon nanofibers for improved cycle life of lithium sulfur batteries, Nano Lett., 13(2013) 1265–1270.

[8] N. Jayaprakash, J. Shen, S. S. Moganty, A. Corona, and L. A. Archer, Porous Hollow Carbon@Sulfur Composites for High-Power Lithium-Sulfur Batteries, Angew. Chem. Int. Ed., 50 (2011) 5904–5908.

[9] J. Shim, K. A. Striebel and E. J. Cairns, The Lithium/Sulfur Rechargeable Cell: Effects of Electrode Composition and Solvent on Cell Performance, J. Electrochem. Soc., 149 (2002) A1321–A1325.

[10] X. Liang, Z. Wen, Y. Liu, M. Wu, J. Jin, H. Zhang, X. Wu, Improved cycling performances of lithium sulfur batteries with LiNO3-modified electrolyte, J. Power Sources, 196(2011) 9839–9843.

[11] B. D. Adams , E. V. Carino, J. G. Connell, K. S. Han , R. Cao , J. Chen , J. Zheng , Q. Li , K. T. Mueller , W. A. Henderson , J.-G. Zhang, Long term stability of Li-S batteries using high concentration lithium nitrate electrolytes, Nano Energy, 40(2017) 607–617.

[12] Y. Yang, G. Zheng and Y. Cui, A membrane-free lithium/polysulfide semi-liquid battery for large-scale energy storage, Energy Environ. Sci., 6(2013) 1552–1558.

[13] Z. Lin and C. Liang, Lithium–sulfur batteries: from liquid to solid cells, J. Mater. Chem. A, 3(2015) 936–958.

[14] A. Hayashi, T. Ohtomo, F. Mizuno, K. Tadanaga, M. Tatsumisago, All-solid-state Li/S batteries with highly conductive glass–ceramic electrolytes, Electrochem. Commun., 5(2003) 701–705.

[15] M. Agostini , Y. Aihara, T. Yamada , B. Scrosati, J. Hassoun, A lithium–sulfur battery using a solid, glass-type P_2S_5–Li_2S electrolyte, Solid State Ionics, 244(2013) 48–51.

[16] R.C. Xu, X.H. Xia, S.Z. Zhang, D. Xie, X.L. Wang , J.P. Tu, Interfacial challenges and progress for inorganic all-solid-state lithium batteries, Electrochim. Acta, 284(2018) 177–187.

[17] C. Sun , J. Liu , Y. Gong, D. P. Wilkinson, J. Zhang, Recent advances in all-solid-state rechargeable lithium batteries, Nano Energy, 33(2017) 363–386.

[18] Q.Wang, J. Jin, X. Wu, G. Ma, J. Yang and Z. Wen, A shuttle effect free lithium sulfur battery based on a hybrid electrolyte, Phys. Chem. Chem. Phys., 16(2014) 21225–21229.

[19] M. Keller, A. Varzi, S. Passerini, Hybrid electrolytes for lithium metal batteries, J. Power Sources, 392(2018) 206–225.

[20] Y. Lu, K. Korf, Y. Kambe, Z. Tu, and L. A. Archer, Ionic-liquid-nanoparticle hybrid electrolytes: applications in lithium metal batteries, Angew. Chem. Int. Ed., 53(2014) 488–492.

[21] O.Sheng, C. Jin, J. Luo, H. Yuan, C. Fang, H. Huang, Y. Gan, J. Zhang, Y. Xia, C. Liang, W.Zhang and X. Tao, Ionic conductivity promotion of polymer electrolyte with ionic liquid grafted oxides for all-solid-state lithium–sulfur batteries, J. Mater. Chem. A, 5(2017) 12934–12942.

Journal Pre-proof

[22] Q. Wang, Z. Wen, J. Jin, J. Guo, X. Huang, J. Yang and C. Chen, A gel-ceramic multi-layer electrolyte for long-life lithium sulfur batteries, Chem. Commun., 52(2016) 1637−1640.

[23] X. Yu, Z. Bi, F. Zhao, and A. Manthiram, Hybrid Lithium–Sulfur Batteries with a Solid Electrolyte Membrane and Lithium Polysulfide Catholyte, ACS Appl. Mater. Interfaces, 7(2015) 16625−16631.

[24] X. Judez, H. Zhang, C. Li, G. G. Eshetu, Y. Zhang, J. A. González-Marcos, M.Armand, and L. M. Rodriguez-Martinez, Polymer-Rich Composite Electrolytes for All-Solid-State Li–S Cells, J. Phys. Chem. Lett., 8(2017) 3473–3477.

[25] X. Yu and A. Manthiram, Electrode–Electrolyte Interfaces in Lithium–Sulfur Batteries with Liquid or Inorganic Solid Electrolytes, Acc. Chem. Res., 50(2017) 2653−2660.

[26] N. Kamaya, K. Homma, Y. Yamakawa, M. Hirayama, R. Kanno, M. Yonemura, T.Kamiyama, Y. Kato, S. Hama, K. Kawamoto and A. Mitsui, A lithium superionic conductor, Nat. Mater., 10(2011) 682–686.

[27] Y. Seino, T. Ota, K. Takada, A. Hayashi and M. Tatsumisago, A sulphide lithium super ion conductor is superior to liquid ion conductors for use in rechargeable batteries, Energy Environ. Sci., 7(2014) 627–631.

[28] P. Bron, S. Johansson, K. Zick, J. S.Günne, S. Dehnen, B. Roling, $Li_{10}SnP_2S_{12}$: An Affordable Lithium Superionic Conductor, J. Am. Chem. Soc., 135(2013) 15694−15697.

[29] C. Yu, S. Ganapathy, E. R. H. van Eck, L. van Eijck,S. Basak, Y. Liu, L. Zhang, H. W. Zandbergen and M. Wagemaker, Li-ion conductivity and solid-state battery performance of the argyrodite Li_6PS_5Br solid electrolyte, J. Mater. Chem. A, 5(2017) 21178–21188.

[30] M. Barghamadi, A. S. Best, A. I. Bhatt, A. F. Hollenkamp, P. J. Mahon, M. Musameh, T. Rüther, Effect of $LiNO_3$ additive and pyrrolidinium ionic liquid on the solid electrolyte interphase in the lithium–sulfur battery, J. Power Sources, 295(2015) 212-220.

[31] S. P. Ong, Y. Mo, W. D. Richards, L. Miara,H. S. Lee and G. Ceder, Phase stability, electrochemical stability and ionic conductivity of the $Li_{10\pm1}MP_2X_{12}$ (M = Ge, Si, Sn, Al or P, and X = O, S or Se) family of superionic conductors, Energy Environ. Sci.,**6(**2013) 148-156.

[32] P. Andrei, C. Shen, J. P. Zheng, Theoretical and experimental analysis of precipitation and solubility effects in lithium-sulfur batteries, Electrochimica Acta, 284(2018) 469–484.

[33] G.-C. Li , G.-R. Li , S.-H. Ye , and X.-P. Gao, A Polyaniline□Coated Sulfur/Carbon Composite with an Enhanced High□Rate Capability as a Cathode Material for Lithium/Sulfur Batteries, Adv. Energy Mater., 2(2012) 1238–1245.

[34] N. Jayaprakash, J. Shen, Surya S. Moganty, A. Corona, and Lynden A. Archer, Porous Hollow Carbon@Sulfur Composites for High□Power Lithium–Sulfur Batteries, Angew. Chem. Int. Ed., 50(2011) 5904–5908.

Journal Pre-proof

[35] C. Wang , Q. Sun, Y. Liu, Y. Zhao , X. Li , X. Lin, M. N.Banis, M. Li, W. Li , K. R. Adair, D. Wang, J. Liang, R. Li, L. Zhang, R. Yang, S. Lu, X. Sun, Boosting the performance of lithium batteries with solid-liquid hybrid electrolytes: Interfacial properties and effects of liquid electrolytes, Nano Energy, 48(2018) 35–43.

[36] W.-G. Lim, C. Jo, A. Cho, J. Hwang, S. Kim, J. W. Han, and J. Lee, Approaching Ultrastable High-Rate Li–S Batteries through Hierarchically Porous Titanium Nitride Synthesized by Multiscale Phase Separation, Adv. Mater. 31(2019), 1806547.

[37] S. Gu, X. Huang, Q. Wang, J. Jin, Q. Wang, Z. Wen and R. Qian, A hybrid electrolyte for long-life semi-solid-state lithium sulfur batteries, J. Mater. Chem. A, 5(2017) 13971–13975.

[38] S. Wang, Y. Ding, G. Zhou, G. Yu, and A. Manthiram, Durability of the $Li_{1+x}Ti_{2-x}Al_x(PO_4)_3$ solid electrolyte in lithium−sulfur batteries, ACS Energy Lett., 1(2016) 1080−1085.

[39] I. Tarhouchi, V. Viallet, P. Vinatier, M. Ménétrier, Electrochemical characterization of $Li_{10}SnP_2S_{12}$: An electrolyte or a negative electrode for solid state Li-ion batteries, Solid State Ionics, 296(2016) 18–25.

[40] Z. Deng, Z. Zhang, Y. Lai, J. Liu, J. Li and Y. Liu, Electrochemical Impedance Spectroscopy Study of a Lithium/Sulfur Battery: Modeling and Analysis of Capacity Fading, J. Electrochem. Soc., 160 (2013) A553–A558.

[41] C. Wang, Y Zhao, Q. Sun, X. Li, Y. Liu, J. Liang, X. Li , X. Lin, R. Li, K. R. Adair, L. Zhang, R. Yang, S. Lub, X. Sun, Stabilizing interface between $Li_{10}SnP_2S_{12}$ and Li metal by molecular layer deposition, Nano Energy, 53(2018) 168–174.

[42] B. Zheng, J. Zhu, H. Wang, M. Feng, E. Umeshbabu, Y. Li, Q.-H. Wu, and Y. Yang, Stabilizing $Li_{10}SnP_2S_{12}$ /Li Interface via an in Situ Formed Solid Electrolyte Interphase Layer, ACS Appl. Mater. Interfaces, 10(2018) 25473−25482.

[43] B. Zheng , X. Liu, J. Zhu, J. Zhao, G. Zhong, Y. Xiang, H. Wang, W. Zhao, E. Umeshbabu, Q.-H. Wu, J. Huang, Y. Yang, Unraveling (electro)-chemical stability and interfacial reactions of $Li_{10}SnP_2S_{12}$ in all-solid-state Li batteries, Nano Energy, 67 (2020) 104252.

[44] J.-W. Park, K. Ueno, N. Tachikawa, K. Dokko, and M. Watanabe, Ionic liquid electrolytes for lithium−sulfur batteries, J. Phys. Chem. C, 117(2013) 20531−20541.

Journal Pre-proof

Journal Pre-proof

An extremely high rate Li-S battery with hybrid electrolyte

Yang-Hai Xu[a,b], Quan-Feng Zhang[a], Bo Fan[a,z], Bai Xue[a], Hui-Jian Chen[a], Xiang-Hua Zhang[a,d], Zhong-Kuan Luo[c], Fang Wang[c], David Le Coq[d], Laurent Calvez [d], Hong-Li Ma[d], Ping Fan[a,z]

[a] Shenzhen Key Laboratory of Advanced Thin Films and Applications, Institute of Thin Film Physics and Applications, College of Physics and Energy, Shenzhen University, 518060 Shenzhen, China.

[b] Key Laboratory of Optoelectronic Devices and Systems of Ministry of Education and Guangdong Province, College of Optoelectronic Engineering, Shenzhen University, Shenzhen 518060, China.

[c] College of Chemistry and Environmental Engineering, Shenzhen University, 3688 Nanhai Avenue, Nanshan District, Shenzhen, 518060, China.

[d] Univ. Rennes, CNRS, ISCR (Institut des Sciences Chimiques de Rennes)-UMR 6226, Rennes, FR 35042.

([z] corresponding author: fanb07@hotmail.com; fanping308@126.com)

High lights

1. $Li_{10}SnP_2S_{12}$ membrane, synthesized at 500 ^oC, is used as both separator and electrolyte with a ceramic-like dense structure and high ionic conductivity of 3.33×10^{-3} S/cm at 25 ^oC.
2. An extremely high rate Li-S battery（5C, 7.1 mA/cm^2）is obtained with hybrid electrolyte.
3. A competitive mechanism exists between the electrochemical reaction and parasitic reaction, where electrochemical reaction dominates at high charge/discharge rates.

Key words: $Li_{10}SnP_2S_{12}$; sulfide solid electrolyte; hybrid electrolyte; Li-S battery; lithium dendrites.

Journal Pre-proof

Journal Pre-proof

Declaration of interests

Dear editor:

The authors declare that they have no known competing financial interests or personal relationships that could have appeared to influence the work reported in this paper.

Your sincerely,

Yang-Hai Xu[a,b], Quan-Feng Zhang[a], Bo Fan[a,z], Bai Xue[a], Hui-Jian Chen[a], Xiang-Hua Zhang[a,d], Zhong-Kuan Luo[c], Fang Wang[c], David Le Coq[d], Laurent Calvez [d], Hong-Li Ma[d], Ping Fan[a,z]

[a] Shenzhen Key Laboratory of Advanced Thin Films and Applications, Institute of Thin Film Physics and Applications, College of Physics and Energy, Shenzhen University, 518060 Shenzhen, China.

[b] Key Laboratory of Optoelectronic Devices and Systems of Ministry of Education and Guangdong Province, College of Optoelectronic Engineering, Shenzhen University, Shenzhen 518060, China.

[c] College of Chemistry and Environmental Engineering, Shenzhen University, 3688 Nanhai Avenue, Nanshan District, Shenzhen, 518060, China

[d] Univ. Rennes, CNRS, ISCR (Institut des Sciences Chimiques de Rennes)-UMR 6226, Rennes, FR 3504 (**z,**corresponding author: fanb07@hotmail.com; fanping308@126.com)

Journal Pre-proof